Therapeutic Targeting of Mesothelin with Chimeric Antigen Receptor T Cells in Acute Myeloid Leukemia

Quy Le[1], Sommer Castro[1], Thao Tang[1], Anisha M. Loeb[1], Tiffany Hylkema[1], Cyd Nourigat McKay[1], LaKeisha Perkins[1], Shivani Srivastava[1], Lindsey Call[1], Jenny Smith[1], Amanda Leonti[1], Rhonda Ries[1], Laura Pardo[1,2], Michael R. Loken[2], Colin Correnti[1], Salvatore Fiorenza[1], Cameron J. Turtle[1,3], Stanley Riddell[1], Katherine Tarlock[1,4], and Soheil Meshinchi[1,4,5]

ABSTRACT

Purpose: We previously identified mesothelin (MSLN) as highly expressed in a significant fraction of acute myeloid leukemia (AML) but entirely silent in normal hematopoiesis, providing a promising antigen for immunotherapeutic targeting that avoids hematopoietic toxicity. Given that T cells genetically modified to express chimeric antigen receptors (CAR) are effective at eradicating relapsed/refractory acute lymphocytic leukemia, we developed MSLN-directed CAR T cells for preclinical evaluation in AML.

Experimental Design: The variable light (VL) and heavy (VH) sequences from the MSLN-targeting SS1P immunotoxin were used to construct the single-chain variable fragment of the standard CAR containing 41-BB costimulatory and CD3Zeta stimulatory domains. The preclinical efficacy of MSLN CAR T cells was evaluated against AML cell lines and patient samples expressing various levels of MSLN *in vitro* and *in vivo*.

Results: We demonstrate that MSLN is expressed on the cell surface of AML blasts and leukemic stem cell–enriched $CD34^{+}CD38^{-}$ subset, but not on normal hematopoietic stem and progenitor cells (HSPC). We further establish that MSLN CAR T cells are highly effective in eliminating MSLN-positive AML cells in cell line– and patient-derived xenograft models. Importantly, MSLN CAR T cells can target and eradicate $CD34^{+}CD38^{-}$ cells without impacting the viability of normal HSPCs. Finally, we show that CAR T-cell functionality can be improved by inhibition of the ADAM17 metalloprotease that promotes shedding of MSLN.

Conclusions: These findings demonstrate that MSLN is a viable target for CAR T-cell therapy in AML and that inhibiting MSLN shedding is a promising approach to improve CAR T-cell efficacy.

Introduction

Acute myeloid leukemia (AML) remains difficult to treat due to high induction failure rates and unacceptable therapy-related toxicities (1–3). Immunotherapy using T cells genetically modified to express chimeric antigen receptors (CAR T) has emerged as a promising approach for treating B-cell leukemias (4, 5); however, its efficacy in AML is yet to be established. Given the limited number of available AML-restricted targets, current approaches target broadly expressed antigens that are shared between normal and leukemic cells (i.e., CD33, CD123; ref. 6), which can lead to significant myelosuppression or myeloablation. In an effort to devise highly specific CAR T-cell therapies that avoid hematopoietic toxicity, we recently completed an extensive discovery effort to identify AML-restricted targets (high expression in AML, absent in normal hematopoiesis). We sequenced the genomes and transcriptomes of nearly 3,000 cases from children and young adults with AML along with a large collection of normal marrow and peripheral blood hematopoietic stem and progenitor cell (HSPC) samples from healthy donors for comparison. Computational analysis of this massive dataset identified mesothelin (MSLN) as a potential therapeutic target in AML as the *MSLN* gene is not expressed in normal marrow and peripheral blood HPSCs but highly expressed in 36% of pediatric AML, including a majority of highly aggressive KMT2A (also known as MLL)-rearranged subset, and 14% (NCI TCGA) in adult AML. Seventy-six percent of patients with *MSLN* gene expression at diagnosis retained the expression at relapse while 4% of *MSLN*-negative patients acquired expression at relapse. Cell surface expression of MSLN on AML blasts is evident in 29% of patients with pediatric AML with median mean fluorescent intensity (MFI) of 34.7 (range, 9.28–498) compared with 5.8 (range, 2.32–14.15) in the MSLN-negative cohort (7). Thus, given the AML-restricted expression, MSLN represents a promising antigen for immunotherapeutic targeting in AML.

Previous studies have shown that MSLN is also highly overexpressed in many solid tumors and that targeting MSLN using a variety of immunotherapeutic strategies demonstrated clinical efficacy with minimal toxicities (8–11). We previously demonstrated effective targeting of MSLN-positive AML cells with antibody–drug conjugates (7). In this study, we assessed the preclinical efficacy of MSLN-directed CAR T cells in AML.

Materials and Methods

Generation of MSLN CAR constructs

CAR constructs containing IgG4 short, intermediate, and long spacers are previously described in ref. 12. The variable light (VL) and heavy (VH) sequences from SS1P immunotoxin (13) were used to construct the anti-MSLN single-chain variable fragment (scFv) with

[1]Fred Hutchinson Cancer Research Center, Seattle, Washington. [2]Hematologics, Inc, Seattle, Washington. [3]Department of Medicine, University of Washington, Seattle, Washington. [4]Department of Pediatrics, University of Washington, Seattle, Washington. [5]Children's Oncology Group, Monrovia, California.

Note: Supplementary data for this article are available at Clinical Cancer Research Online (http://clincancerres.aacrjournals.org/).

Corresponding Author: Quy Le, Clinical Research Division, Fred Hutchinson Cancer Research Center, Seattle, WA, 98109. Phone: 206-667-6008; Fax: 206-667-6084; E-mail: quyl@fredhutch.org

Clin Cancer Res 2021;27:5718–30

doi: 10.1158/1078-0432.CCR-21-1546

Translational Relevance

We previously identified mesothelin (MSLN) as a viable therapeutic target in acute myeloid leukemia (AML) by sequence analysis of nearly 3,000 AML cases and a large collection of normal counterparts. Here, we report development, optimization, and assessment of the preclinical efficacy of CAR T cells directed against MSLN in AML. We show that the cell surface expression of MSLN is restricted to AML blasts and leukemic stem cell–enriched $CD34^+CD38^-$ subset but absent in normal hematopoietic stem and progenitor cells. We demonstrate that MSLN-directed CAR T cells exhibit potent, target-specific cytotoxicity against AML cells *in vitro* and *in vivo* and can effectively eliminate $CD34^+CD38^-$ cells without compromising normal hematopoietic stem and progenitor cells. Moreover, treatment with the metalloprotease inhibitor GM6001 enhances this killing capacity by stabilizing MSLN on the cell surface. These results establish the therapeutic potential of MSLN-directed CAR T cells and support testing in clinical trials for AML.

VL/VH orientation using G4SX4 linker. Anti-MSLN single-chain variable fragment (scFv) DNA fragment was human codon optimized and synthesized by IDT gBlock gene fragment and cloned into the CAR vectors with *Nhe*I and *Rsr*II restriction sites upstream of the IgG4 spacer.

SS1 scFv

DIELTQSPAIMSASPGEKVTMTCSASSSVSYMHWYQQKSGTSPKRWIYDTSKLASGVPGRFSGSGSGNSYSLTISSVEAEDDATYYCQQWSGYPLTFGAGTKLEIKGGGGSGGGGSGGGGSGGGGSQVQLQQSGPELEKPGASVKISCKASGYSFTGYTMNWVKQSHGKSLEWIGLITPYNGASSYNQKFRGKATLTVDKSSSTAYMDLLSLTSEDSAVYFCARGGYDGRGFDYWGQGTTVTVSS.

Generation of human MSLN CAR T cells

CAR T cells were generated by transducing healthy donor T cells (Bloodworks Northwest) with lentivirus carrying the CAR vector under the approval of FHCRC Institutional Review Board (protocol #9950). Peripheral blood mononuclear cells from healthy donors were isolated over Lymphoprep (StemCell Technologies, catalog no. 07851). CD4 or CD8 T cells were isolated by negative magnetic selection using Easy Sep Human CD4+ T cell Isolation Kit II (StemCell Technologies, catalog no. 17952) and Easy Sep Human CD8+ T cell Isolation Kit II (StemCell Technologies, catalog no. 17953). Purified T cells were cultured in CTL media [RPMI supplemented with 10% human serum (Bloodworks Northwest), 2% L-glutamine (Gibco, catalog no. 25030–081), 1% penicillin-streptomycin (Gibco, catalog no. 15140–122), 0.5 mol/L β-mercaptoethanol (Gibco, catalog no. 21985–023), and 50 U/mL IL2 (aldesleukin, Prometheus)] at 37°C in 5% CO_2. T cells were activated with anti-CD3/CD28 beads (3:1 beads: cell, Gibco, 11131D) on Retronectin-coated plates (5 μg/mL, coated overnight at 4°C; Takara, catalog no. T100B) and transduced with CAR lentivirus (MOI = 50) one day after activation via spinoculation at 800 × *g* for 90 minutes at 25°C in CTL media (+50 U/mL IL2) supplemented with 8 μg/mL protamine sulfate. Transduction used 200,000 cells per well in 24-well plates. Transduced cells were expanded in CTL media (+50 U/mL IL2) and separated from beads on day 5. As truncated CD19 was coexpressed with the CAR by a T2A ribosomal skip element, it was used to select for transduced cells. Transduced cells were sorted for CD19 expression [using anti-human CD19 PE (BioLegend, catalog no. 982402)] on FACSAria II 8–10 days postactivation. Sorted cells were further expanded in CTL (+50 U/mL IL2) media for an additional 4–6 days prior to *in vitro* and *in vivo* cytotoxicity assays.

Cell lines and GM6001 treatment

Nomo-1 and Kasumi-1 cell lines were obtained from ATCC and maintained per manufacturer's instructions. We engineered Kasumi-1 $MSLN^+$ cell line by transducing Kasumi-1 cells with a lentivirus containing the *MSLN* transgene driven by the EF1a promoter (see ref. 7). Jurkat Nur77 reporter cells were maintained in RPMI supplemented with 20% FBS and 2 mmol/L L-Glutamine.

GM6001 (Selleckchem, catalog no. S7157) is a matrix metalloprotease inhibitor. It is stable *in vitro*, but its half-life of *in vivo* is reported to be <15 minutes (ref. 14; and see details at https://www.emdmillipore.com/US/en/product/GM6001-MMP-Inhibitor,MM_NF-CC1010). Nomo-1 cells were treated with GM6001 (50 μmol/L) or DMSO control for 48 hours prior to evaluation of surface MSLN by flow cytometry; of soluble MSLN in the culture supernatant by ELISA; and of cell lysis activity by coculture with MSLN CAR T cells. For *in vitro* cytotoxicity assay, fresh GM6001 (50 μmol/L) or DMSO was added to the coculture of Nomo-1 and CAR T cells. For *in vivo* assays, mice were treated with GM6001 at 100 mg/kg once a day for 3–7 days via intraperitoneal injection.

Primary samples

Frozen aliquots of mononuclear $CD45^+$ cells isolated from AML diagnostic bone marrow samples were obtained from the Children's Oncology Group (see **Table 1** for additional information). Frozen aliquots of CD34-enriched bone marrow samples were obtained from FHCRC Cooperative Centers of Excellence in Hematology Core B. Cells were thawed in IMDM supplemented with 20% FBS and 100 U/mL DNaseI (Sigma, catalog no. D5025) and placed directly into the T-cell killing assay or transplanted into NSG-SMG3 mice for *in vivo* efficacy assessment. A small aliquot of freshly thawed cells was used to assess expression of MSLN and LSC/HSC markers (see Supplementary Information). For some samples, cells were sent to Hematologics, Inc. for immunophenotype analysis of MSLN cell

Table 1. Biologic and disease characteristics of AML patient specimens.

	Sex	Age (yrs)	% blasts in bone marrow	Primary cytogenetic	Primary fusion	FLT3/ITD?	WT1?	NPM1?	CEBPA?
Patient 1	Female	2	61	Unknown	Unknown	Unknown	Unknown	Unknown	Unknown
Patient 2	Female	11	84	Unknown	Unknown	Unknown	Unknown	Unknown	Unknown
Patient 3	Female	18	85	inv(16)	CBFB-MYH11	No	No	No	No
Patient 4	Female	17	83	MLL	KMT2A-MLLT3	No	No	No	No
Patient 5	Male	1	91	MLL	KMT2A-MLLT10	No	No	No	No
Patient 6	Female	15	90	Normal	None	No	No	No	Yes

surface expression. All specimens used in this study were obtained after written content from patients and donors. The research was performed after approval by the FHCRC Institutional Review Board (protocol #9950). The study was conducted in accordance with the Declaration of Helsinki.

In vitro studies

Target cells (Nomo-1, Kasumi-1 *MSLN*$^+$, and Kasumi-1 parental) were split 1–2 days prior to cytotoxicity assay. Target cells using primary samples were thawed and used directly in the cytotoxicity assay. Target leukemia cells were labeled with 2.5 μmol/L CFSE (Invitrogen, catalog no. C34554) as per manufacturer's directions, washed with 1X PBS, and resuspended in CTL media (without IL2). For T-cell proliferation assay, effector cells (unmodified or MSLN CAR T cells) were labeled with 2.5 mol/L Violet Cell Proliferation Dye (Invitrogen, catalog no. C34557) washed with 1X PBS, serial diluted in CTL media (without IL2), and combined with target cells at various effector:target (E:T) ratios in 96 U-bottom plate. Cytotoxicity (at indicated time points) and T-cell proliferation (4 days) were assessed by flow cytometry after staining cells with live/dead fixable viability dyes [FVD; Invitrogen, catalog no. L34964 (cytotoxicity) or L10120 (T-cell proliferation)]. Percent dead among target cells was assessed by gating on FVD$^+$ among CFSE$^+$ target cells. Percent-specific lysis was calculated by subtracting the average of the three replicate wells containing target cells only from each well containing target and effector cells at each E:T ratio. After 24 hours of coculture, media supernatant were assessed for IL2, IFNγ, and TNFα production by Luminex microbead technology (provided by FHCRC Immune Monitoring Core).

In vivo studies

For cell line–derived xenograft (CDX) models, we transduced Nomo-1, Kasumi-1 *MSLN*$^+$, and Kasumi-1 parental cells with GFP/ffluciferase construct (Plasmid #104834, Addgene) and sorted for GFP$^+$ cells. Luciferase-expressing cells were injected intravenously into NSG mice through the tail vein at 10^6 cells per mouse. Mice were treated with MSLN CAR T or unmodified T cells via tail vein intravenous injection 1 week following Nomo-1 injection and 2 weeks following Kasumi-1 *MSLN*$^+$ and Kasumi-1 parental injections. Leukemia burden was measured by bioluminescence imaging weekly. For the patient-derived xenograft (PDX) model, cells derived from patient 5 were injected into NSG-SGM3 mice (10^6 cells/mouse) followed by T cells (5×10^6 cells/mouse) 4 days later via tail vein intravenous injection. Leukemia burden and T-cell expansion were monitored by flow cytometric analysis of mouse peripheral blood, which was drawn by retro-orbital bleeds for the indicated time points starting from the first week of T-cell injection, and mouse bone marrow, which was aspirated at the indicated time point post T-cell injection. Mice were monitored and euthanized when they exhibited symptomatic leukemia (tachypnea, hunchback, persistent weight loss, fatigue, or hind-limb paralysis). Tissues such as blood, bone marrow, liver, spleen, and tumors were harvested at necropsy and analyzed for the presence of T and leukemia cells. This study was performed after approval by FHCRC IACUC (protocol #51068).

Flow cytometry of xenograft cells

Mouse bone marrow, spleen, liver, and tumors were harvested at necropsy and passed through a 70-μm cell strainer to dissociate tissues into single cells prior to antibody staining. Cells from mouse peripheral blood were processed with red blood cell lysis buffer, washed in 2% FBS in PBS, blocked with 20 ug/mL Fc receptor block (BD Pharmingen, catalog no. 564219) in PBS, then stained with a cocktail of fluorescently labeled mAbs that included a combination of APC/Cyanine 7-conjugated anti-mouse CD45.1 (BioLegend, catalog no. 110716), BUV805-conjugated anti-human CD45 (BD Biosciences, catalog no. 612891), APC-conjugated anti-human CD19 (BD Biosciences, catalog no. 555415), PE-Cy7–conjugated anti-human CD3 (BD Biosciences, catalog no. 563423), Brilliant Violet 605–conjugated anti-human CD4 (BioLegend, catalog no. 317438), BV711-conjugated anti-human CD8 (BD Biosciences, catalog no. 563677), PerCP/Cyanine 5.5-conjugated anti-human CD33 (BioLegend, catalog no. 303414), and PE-conjugated anti-human MSLN (amatuximab, FHCRC; see ref. 7 for the generation of this antibody) for 20 minutes on ice. Labeled cells were washed with PBS and resuspended in 2% FBS/PBS prior to flow cytometric analysis. LSR Fortessa X50 equipped with FACSDiva Software (BD Biosciences) was used to assess cell surface expressions and FlowJo Software was used for the analysis. Dead cells were excluded based on DAPI staining.

Statistical analysis

Unpaired, two-tailed Student *t* test was used to determine statistical significance for all *in vitro* studies. Log-rank (Mantel–Cox) test was used to compare Kaplan–Meier survival curves between experimental groups. *P* values <0.05 were statistically significant.

Results

MSLN is expressed on the AML leukemic stem cell–enriched CD34$^+$CD38$^-$ subset

To determine whether MSLN is expressed on leukemic stem cells (LSC), we first determined the fraction of LSCs of the CD34$^+$CD38$^-$ phenotype in primary cells from 5 MSLN-positive patients, and found 12%, 28%, and 1.3% in patients 1–3, respectively, with undetectable frequencies in patients 4 and 5 (**Fig. 1A**, top). We then characterized MSLN expression on the LSC-enriched population (CD34$^+$CD38$^-$) from patients 1–3 in comparison with normal marrow HSPCs from 3 healthy donors (**Fig. 1A**, bottom). In each of these patients, MSLN expression was comparable in the LSC-enriched population and the bulk population (**Fig. 1B**, top). In contrast, in samples from healthy donors, MSLN expression was entirely silent in hematopoietic stem cells (HSC), multipotent progenitors (MPP), multi-lymphoid progenitors (MLP), common lymphoid progenitors (CLP), megakaryocyte-erythroid progenitors (MEP), common myeloid progenitors (CMP), and granulocyte monocyte progenitors (GMP; **Fig. 1B**, bottom). Quantification with additional patient samples revealed that a high fraction of cells in both the bulk and LSC-enriched subset were MLSN-positive cells in the majority of these patients (70.4 $\pm$ 24.0% and 67.1 $\pm$ 26.6%, respectively; $N = 14$; **Fig. 1C**), and these cells exhibited corresponding higher MFI as compared with the normal HSPC subsets (**Fig. 1D**). These results suggest that targeting MSLN may provide a strategy to eliminate LSCs without impacting normal hematopoiesis.

MSLN CAR with a short IgG4 hinge domain confers superior cytotoxicity over intermediate and long IgG4 domains

To evaluate the therapeutic potential of targeting MSLN, we generated MSLN-directed CARs by fusing the single-chain variable fragment derived from the SS1P immunotoxin (13) to the IgG4 spacer, CD28 transmembrane, 4–1BB costimulatory, and CD3ζ signaling domains (12, 15). As the length of the spacer domain affects the distance between the CAR and its target antigen and is known to

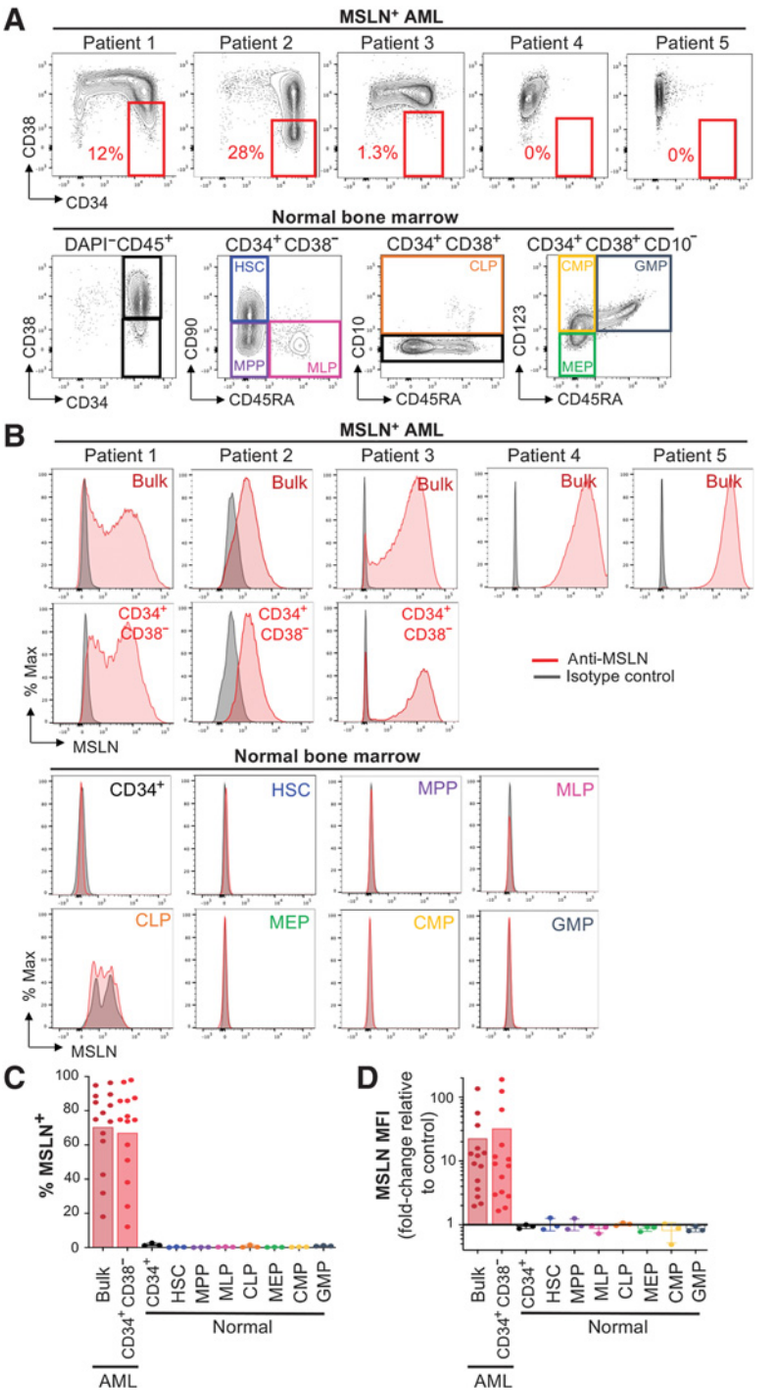

Figure 1.

MSLN is expressed on LSC-enriched $CD34^+CD38^-$ subset, but not on normal HSPCs. **A,** Gating strategy used to identify LSCs based on CD34 and CD38 expression in 5 MSLN-positive AML samples (top) and HPSC subsets from a representative CD34-enriched marrow sample from a healthy donor (bottom). Immunophenotype of the HSPCs is as follows: $CD34^+CD38^-CD90^+CD45RA^-$ (hematopoietic stem cell, HSC); $CD34^+CD38^-CD90^-CD45RA^-$ (multipotent progenitors, MPP); $CD34^+CD38^-CD90^-CD45RA^+$ multi-lymphoid progenitors, MLP); $CD34^+CD38^+CD10^+$ (common lymphoid progenitors, CLP); $CD34^+CD38^+CD10^-$-$CD123^-CD45RA^-$ (megakaryocyte-erythroid progenitors, MEP); $CD34^+CD38^+CD10^-CD123^+CD45RA^-$ (common myeloid progenitors, CMP); $CD34^+CD38^+CD10^-CD123^+CD45RA^+$ (granulocyte monocyte progenitors, GMP). **B,** Histograms of MSLN expression in AML bulk, AML $CD34^+CD38^-$, and normal HSPC subsets. **C** and **D,** Quantification of percent $MSLN^+$ (**C**) and MSLN MFI (**D**) across indicated subsets for Patients 1–3 and additional 11 MSLN-positive patient samples containing the $CD34^+CD38^-$ subset as well as 3 healthy donor CD34-enriched marrow samples. Bar indicates the mean. The additional 11 patient samples were sent to Hematologics, Inc. to assess the MSLN expression on the $CD34^+CD38^-$ subset using the same anti-MLSN PE-conjugated antibody used in this study. Autofluorescence was used as a control for these samples. For Patients 1–3, PE-conjugated isotype control (see Material and Methods) was used to define MSLN-positive cells.

influence CAR function (16, 17), we optimized the spacer region (short, intermediate, and long; **Fig. 2A**) and determined that the MSLN CAR with the short hinge domain conferred superior cytotoxicity compared with CARs with intermediate and long spacers (**Fig. 2B**). To determine whether the CAR constructs exhibit tonic or constitutive signaling, we assayed NFAT, NFκB, and AP-1 expression in Jurkat Nur77 reporter cells (18) transduced with the CAR constructs and cultured alone or cocultured in the presence of Kasumi-1 cells engineered to express MSLN (Kasumi-1 *MSLN*$^+$). None of the MSLN CAR constructs demonstrated tonic or constitutive signaling in the absence of target binding (**Fig. 2C** and **D**).

MSLN-directed CAR T cells demonstrate potent cytotoxicity *in vitro* and *in vivo*

Using the MSLN CAR construct with the short hinge domain, we tested the target specificity of MSLN CAR T cells against Nomo-1, which expresses endogenous MSLN; Kasumi-1, which does not express MSLN; and Kasumi-1 engineered to express MSLN

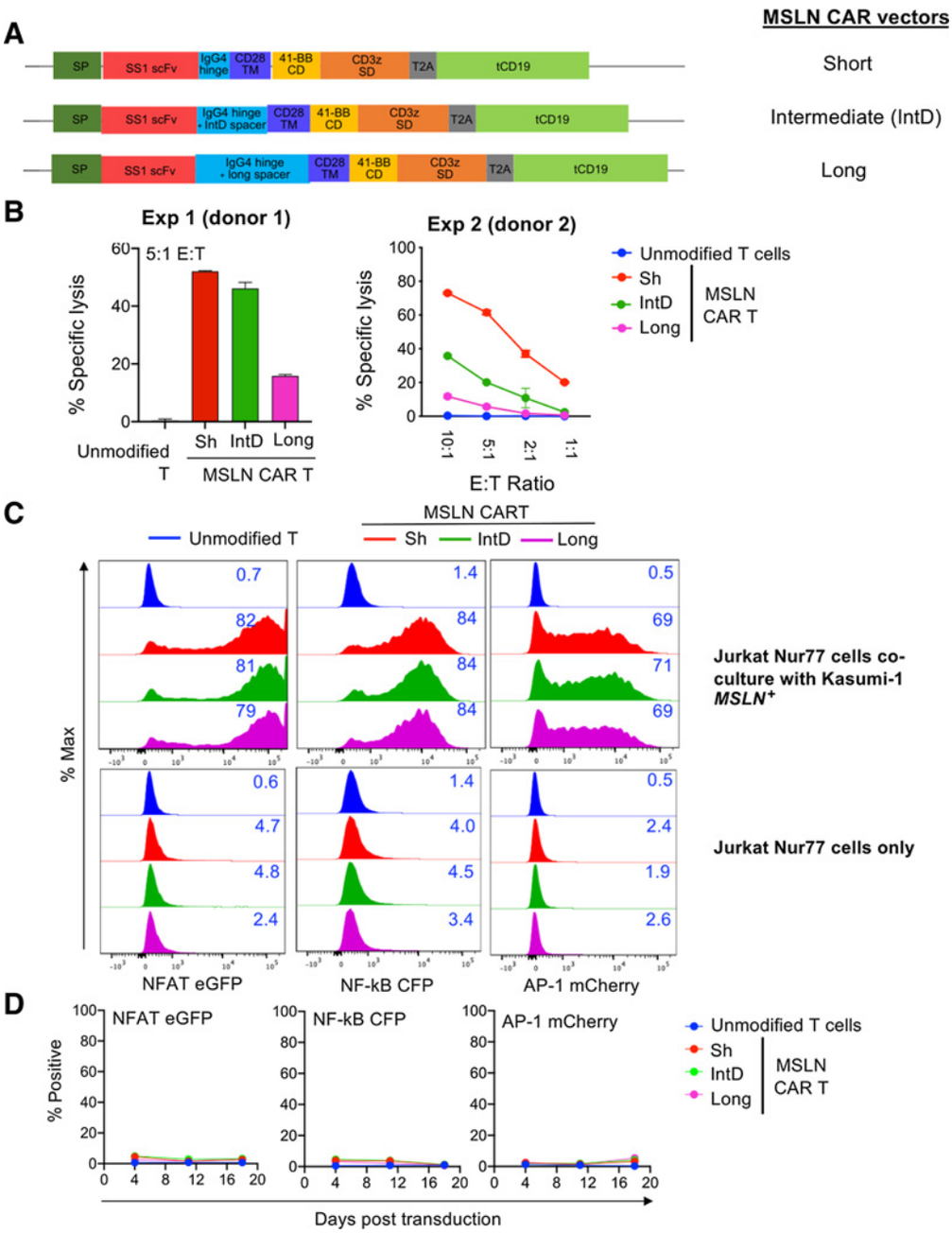

Figure 2.

MSLN CAR constructs and cytolytic activity of short, intermediate, and long MSLN CAR T cells. **A,** Schematic diagram of second-generation MSLN CAR constructs with different IgG4 spacer lengths. CD, costimulatory domain; SD, stimulatory domain; SP, GM-CSFR signal peptide; tCD19, truncated CD19; TM, transmembrane domain. **B,** Cytolytic activity of CD8 T cells unmodified or transduced with short, intermediate, or long MSLN CAR construct against Kasumi-1 *MSLN*$^+$ cells in a 4-hour assay. Data presented are mean percent specific lysis ± SD from three technical replicates at indicated Effector:Target (E:T) ratios. **C,** Representative flow plots showing expression of NFAT, NFκB, and AP-1 in Jurkat Nu77 reporter transduced with MSLN CAR constructs cultured alone (bottom) or coincubated with Kasumi-1 *MSLN*$^+$ target cells (top). Analysis was performed on day 4 posttransduction. Number in top right corner indicates the percentage of positive cells. **D,** Quantification of percent NFAT$^+$, NFκB$^+$, and AP-1$^+$ cells over days posttransduction.

(Kasumi-1 *MSLN*$^+$; **Fig. 3A**). CD8 MSLN CAR T cells demonstrated potent cytolytic activity against Nomo-1 and Kasumi-1 *MSLN*$^+$ cells but not Kasumi-1 parental cells (**Fig. 3B**; Supplementary Fig. S1A). To further evaluate target specificity, we measured cytokine production and cell proliferation of MSLN CAR T and unmodified control T cells following coculture with target cells. Following coculture with Nomo-1 and Kasumi-1 *MSLN*$^+$ cells, but not Kasumi-1 parental cells, both CD8 and CD4 MSLN CAR T cells produced higher levels of IL2, IFNγ, and TNFα than did unmodified T cells (**Fig. 3C**; Supplementary Fig. S1B). Furthermore, both CD8 and CD4 MSLN CAR T cells proliferated

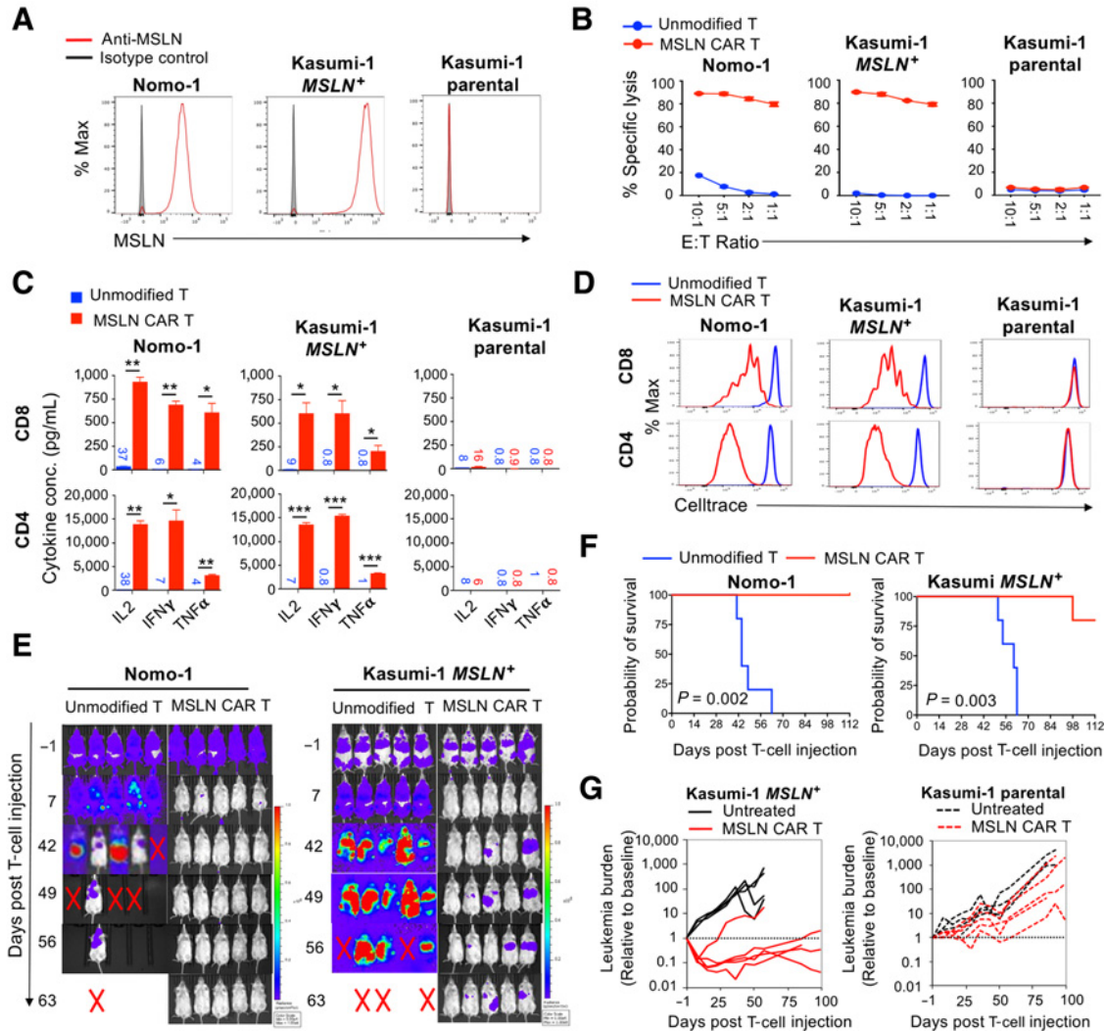

Figure 3.

Target-specific reactivity of MSLN CAR T cells with MSLN-positive AML cell lines. **A,** Flow cytometric analysis of MSLN expression in Nomo-1, Kasumi-1 *MSLN*$^+$, and Kasumi-1 parental cells (red) compared with isotype control (black). **B,** Cytolytic activity of CD8 T cells unmodified or transduced with MSLN CAR following 24 hours of coculture with Nomo-1 and 10 hours with Kasumi-1 *MSLN*$^+$ and Kasumi-1 parental cells. Data presented are mean leukemia specific lysis ± SD from three technical replicates at indicated E:T ratios. Data are representative of three donors (see related data in Supplementary Fig. S1A). **C,** Concentration of secreted IL2, IFN**γ**, and TNF**α** in the supernatant following 24 hour of T-cell/AML coculture at 1:1 E:T ratio as measured by ELISA. Data are representative of two donors and are presented as mean ± SD from three technical replicates (see related data in Supplementary Fig. S1B). Where concentrations of cytokines are too low to discern, the number above the *x*-axis indicates the average concentration. Statistical significance was determined by unpaired Student *t* test, assuming unequal variances. $P < 0.05$ (*), $P < 0.005$ (**), $P < 0.0005$ (***). **D,** Representative flow cytometric analysis of cell proliferation of Cell Proliferation Dye–labeled unmodified and MSLN CAR T cells after 4-day coculture with target cells at 1:1 E:T ratio (see related data in Supplementary Fig. S2). Data are representative of 2 donors. **E,** Bioluminescent imaging of Nomo-1 and Kasumi-1 MSLN$^+$ leukemias in mice treated with unmodified or MSLN CAR T cells at 7.5×10^6 (Nomo-1) or 5×10^6 (Kasumi-1 *MSLN*$^+$) T cells per mouse. $N = 5$ mice per group. **F,** Kaplan–Meier survival curves of Nomo-1 and Kasumi *MSLN*$^+$ xenografts treated with unmodified or MSLN CAR T cells. $N = 5$ per group. **E** and **F,** Data are representative of two independent experiments with T cells derived from two separate donors. **G,** Analysis of Kasumi-1 *MSLN*$^+$ and Kasumi-1 xenografts untreated or treated with 5×10^6 MSLN CAR T cells/mouse (separate experiment with different donor T cells than shown in **E** and **F**), quantifying leukemia burden over time. Data are plotted relative to baseline [one day before CAR T-cell injection (day −1)]. Leukemia burden is shown for each mouse. $N = 5$ mice per group. Statistical differences in survival were evaluated using log-rank Mantel–Cox.

robustly in the presence of Nomo-1 and Kasumi-1 *MSLN*$^+$ cells, but not Kasumi-1 parental cells (**Fig. 3D**; Supplementary Fig. S2). These results indicate highly specific reactivity of MSLN CAR T cells against AML cells engineered to express MSLN or expressing endogenous level of MSLN.

We next investigated the ability of MSLN CAR T cells to eradicate AML *in vivo*. Nomo-1 and Kasumi-1 MSLN$^+$ cells stably expressing luciferase were injected into NSG mice, and once leukemic engraftment was established the leukemia-bearing mice were treated with unmodified T or MSLN CAR T cells. Treatment with MSLN CAR T cells induced leukemia clearance within a week of infusion in both Nomo-1 and Kasumi-1 *MSLN*$^+$ xenograft models; remarkably, leukemia clearance was maintained in the Nomo-1 mice for the entire duration of the study (112 days; **Fig. 3E**). In contrast, all mice that

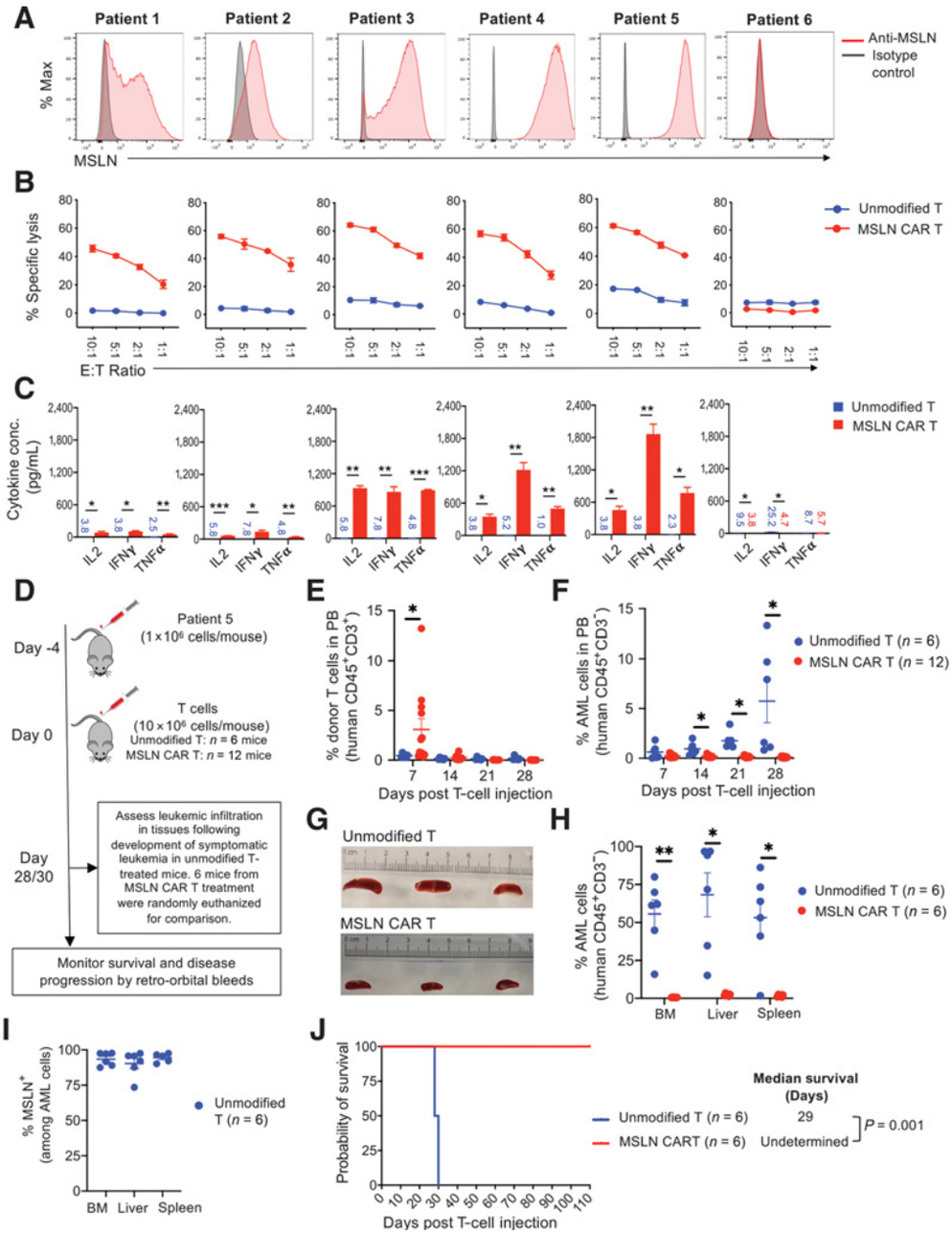

Figure 4.

Preclinical efficacy of MSLN CAR T cells against primary MSLN-positive AML cells. **A,** Flow cytometric analysis of MSLN expression in 6 AML patient samples. **B,** Cytolytic activity of CD8 T cells unmodified or transduced with MSLN CAR following 4-hour coculture with primary AML cells. **C,** Concentration of secreted IL2, IFNγ, and TNFα in the supernatant following 24 hours of CD4 T-cell/AML coculture at 1:1 E:T ratio as measured by ELISA. Where concentrations of cytokines are too low to discern, the numbers above the *x*-axis indicate the average concentration. **B** and **C,** Data are representative of two donors (except for patient 4, which was not repeated) and are presented as mean ± SD from three technical replicates. **D,** Experimental design evaluating *in vivo* MSLN CAR T activity against primary AML cells from patient 5. Mice were treated with 1×10^7 T cells per mouse. **E** and **F,** Quantification of the percent donor T and AML cells in the peripheral blood following days post T-cell injection. $n = 6$ (Unmodified T) and $n = 12$ (MSLN CAR T). **G,** Spleens harvested from control mice at necropsy following development of leukemia (28 and 30 days post T-cell injection) as well as from 6 MSLN CAR T cell–treated mice selected at random 30 days post T-cell injection. $n = 6$ per group. **H,** Percent AML cells in the bone marrow, liver, and spleen from mice described in **G**. **I,** Percent $MSLN^+$ cells among AML cells in the bone marrow (BM), liver, and spleen from mice treated with unmodified T cells at necropsy. One control mouse did not have human engraftment in the spleen. **E, F, H, I,** Data are presented as mean ± SEM. **C, E, F, H,** Statistical significance was determined by unpaired Student *t* test, assuming unequal variances. $P < 0.05$ (*), $P < 0.005$ (**), $P < 0.0005$ (***). **J,** Kaplan–Meier survival curves of PDX mice treated with unmodified or MSLN CAR T cells. Statistical differences in survival were evaluated using log-rank Mantel–Cox.

received unmodified T cells exhibited disease progression with a median survival of 37 days ($P < 0.002$; **Fig. 3F**, left). Likewise, in Kasumi-1 *MSLN*$^+$ xenograft model, treatment with MSLN CAR T cells significantly reduced leukemia burden, and 4 of 5 mice survived until study endpoint at day 112, whereas median survival of mice treated with unmodified T cells was 56 days ($P = 0.003$; **Fig. 3F**, right). Activity of MSLN CAR T cells *in vivo* was target specific, as they did not limit the progression of Kasumi-1 parental cells in NSG mice (**Fig. 3G**). Consistent with enhanced antitumor activity, T cells expanded rapidly in the peripheral blood of CAR-T cell–treated Nomo-1 and Kasumi-1 *MSLN*$^+$ leukemia-bearing mice, with >80% of CD4 and >60% of CD8 T cells expressing the tCD19 transduction marker at day 12 post T-cell injection (Supplementary Fig. S3).

MSLN-directed CAR T cells demonstrate preclinical efficacy against primary MSLN-positive AML cells

To investigate whether MSLN CAR T cells can effectively eliminate primary AML cells, we tested their cytolytic activity on 5 MSLN-positive patient samples (same samples that were described in **Fig. 1**) and 1 MSLN-negative patient sample *in vitro*. The 5 MSLN-positive patient samples expressed different levels of MSLN (**Fig. 4A**) but all were sensitive to the cytolytic activity of MSLN CAR T cells; viability of the MSLN-negative patient sample was unaffected following 4-hour coincubation with MSLN CAR T cells as compared with coincubation with unmodified control T cells (**Fig. 4B**). Furthermore, MSLN CAR T cells produced increased levels of IL2, IFNγ, and TNFα proinflammatory cytokines compared to unmodified control T cells in the presence of MSLN-positive samples but not the MSLN-negative sample (**Fig. 4C**). Thus, MSLN CAR T cells exhibit target-specific reactivity against primary AML cells *in vitro*.

To determine whether MSLN CAR T cells exhibit *in vivo* efficacy against primary AML cells, we developed a PDX model using bone marrow cells from patient 5 (KMT2A-rearranged positive; see **Table 1**). These cells provided a robust model system to evaluate the *in vivo* activity of MSLN CAR T cells, as they produced an aggressive leukemia in humanized NSG-SGM3 mice with median survival of 42, 28, and 27 days in primary, secondary, and tertiary transplants, respectively, accompanied by significant infiltration into the bone marrow, liver, and spleen (Supplementary Fig. S4A and S4B). Leukemic cells harvested from the bone marrow, liver, spleen, and peripheral blood following the development of symptomatic leukemia in primary, secondary, and tertiary transplants showed high level and almost uniform expression of MSLN, comparable with that of cells from a freshly thawed aliquot (Supplementary Fig. S4C and S4D). The leukemic burden of PDX NSG-SGM3 mice was assessed by flow cytometric analysis of AML cells in the peripheral blood and bone marrow aspirates following treatment with unmodified control or MSLN CAR T cells at 1×10^7 T cells per mouse (**Fig. 4D**). The CAR T cells, but not unmodified T cells, expanded by day 7 and then subsided by day 14 following T-cell injection, as evident by the fraction of donor T cells in the peripheral blood (**Fig. 4E**). Remarkably, by day 14 following T-cell injection, AML cells were undetectable in the peripheral blood of mice treated with CAR T cells, whereas significant engraftment had occurred in mice treated with unmodified control T cells that progressed until mice developed symptomatic leukemia following 28–30 days post T-cell injection (**Fig. 4F**). At necropsy of control mice, enlarged spleens were observed (**Fig. 4G**). Further consistent with the anti-leukemia activity of MSLN CAR T cells, no detectable engraftment of AML cells was evident in the bone marrow, liver, and spleen 30 days post T-cell injection from mice treated with CAR T cells, whereas significant engraftment in these tissues had occurred in mice treated with unmodified T cells following development of symptomatic leukemia (**Fig. 4H**). Leukemia cells that infiltrated the bone marrow, spleen, and liver of control mice had uniform expression of MSLN (**Fig. 4I**). Importantly, the MSLN CAR T cells enhanced the survival of the PDX mice ($P = 0.001$; **Fig. 4J**).

To determine whether MSLN CAR T cells were effective at a lower dose, we treated the PDX mice with 5×10^6 T cells per mouse (Supplementary Fig. S5A). Similar leukemia clearance was observed as in the experiment with the higher T-cell dose (Supplementary Fig. S5B–S5D); however, the median survival of PDX mice only increased from 21 to 59 days following treatment with MSLN CAR T cells ($P = 0.025$; Supplementary Fig. S5E). MSLN was expressed in the AML cells harvested from the tissues at necropsy in unmodified T-cell–treated mice as well as CAR T-cell–treated mice that had relapsed (Supplementary Fig. S5F and S5G). Of note, chloromas (solid extramedullary tumors, EMD) were detected in CAR T-cell–treated mice that relapsed (Supplementary Fig. S5F and S5G). Donor T cells were not detected in the unmodified T-cell–treated mice at necropsy and in the CAR T-cell–treated mice at relapse (Supplementary Fig. S5H). Collectively, these results demonstrate the lytic activity of MSLN CAR T cells in eradicating primary AML cells both *in vitro* and *in vivo*.

MSLN-directed CAR T cells effectively eliminate MSLN-positive CD34$^+$CD38$^-$ cells without impacting the viability of normal HSCs

Given that MSLN is expressed on AML CD34$^+$CD38$^-$ cells but not normal HSPCs, we hypothesized that the MSLN CAR T cells would exhibit cytolytic activity against MSLN-positive LSCs, but not normal HSPCs. We tested this by comparing the cytolysis of CD34$^+$CD38$^-$ cells from patients 1–3 (see **Fig. 1** for MSLN expression) and normal marrow HSPCs from 3 healthy donors. After 4 hours of coculture, MSLN CAR T cells demonstrated comparable cytolytic activity against CD34$^+$CD38$^-$ cells and bulk AML from all 3 patients (**Fig. 5A**; Supplementary Figs. S6 and S7) and eliminated almost the entire MSLN-positive cells within the bulk and LSC-enriched populations (**Fig. 5B**; Supplementary Fig. S7B), suggesting highly potent activity. No cytolytic activity was detected against normal HSCs, MPPs, MLPs, CLPs, MEPs, CMPs, and GMPs at 4 hours (**Fig. 5A**) and against CD34$^+$ cells at 4 and 24 hours (Supplementary Fig. S8). Moreover, MSLN CAR T cells did not affect the self-renewal and multilineage differentiation capacity of normal HSPCs as compared with unmodified control T cells (**Fig. 5C**). Together, these results suggest that MSLN CAR T cells can eradicate LSCs without compromising normal HSPCs.

Modulating MSLN shedding improves the efficacy of MSLN-directed CAR T cells

MSLN is actively cleaved from the cell membrane (shedding), which contributes to a pool of soluble MSLN circulating in the blood and may hinder antibody-based therapies (19–21). Shedding reduces antigen site density and may promote the dissociation of CAR bound to MSLN from the cell surface (22). Soluble antigen can also limit CAR T-cell functionality by competing for the antigen binding domain of the CAR as observed with BCMA CAR T cells (23). The well-characterized "sheddase" ADAM17 (TACE), which is responsible for the release of many membrane-bound proteins (24), is implicated in chemotherapy resistance (25, 26). MSLN is a target of ADAM17 cleavage, and inhibiting ADAM17 activity with the pan-metalloproteinase inhibitor GM6001 (20, 21) or by mutating the ADAM17 cleavage site (19) leads to increased MSLN, cell surface density, decreased production of

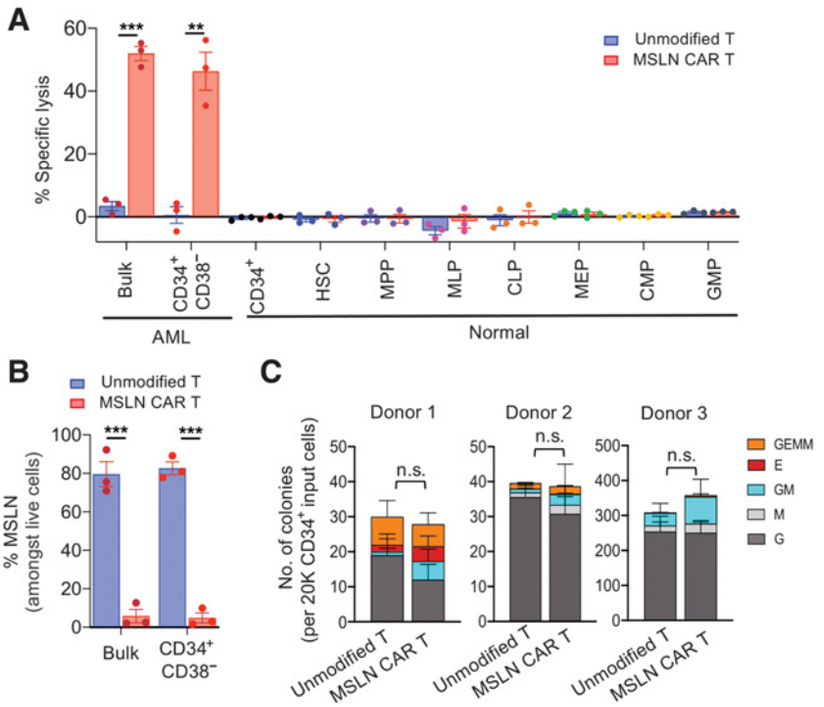

Figure 5.

MSLN CAR T cells effectively eliminate AML $CD34^+CD38^-$ cells but exhibit no cytolytic activity against normal HSCs. **A,** Quantification of percent specific lysis in AML bulk population and LSCs across three AML samples (Patients 1–3) and HSPC subsets from three CD34-enriched bone marrow samples from healthy donors following 4-hour incubation with unmodified or MSLN CAR T cells at 2:1 E:T ratio. **B,** Percent $MSLN^+$ cells among surviving AML bulk and LSCs (FVD−) after coincubation for 4 hours with unmodified or MSLN CAR T cells at 2:1 E:T ratio. Data are presented as mean ± SEM from 3 samples (**A** and **B**). See Supplementary Fig. S6 for the flow cytometric analysis. Experiment shown in A and B was repeated with T cells from another healthy donor and similar results were obtained (Supplementary Fig. S7). Statistical significance was determined by unpaired Student *t* test, assuming unequal variances. $P < 0.05$ (*), $P < 0.005$ (**), $P < 0.0005$ (***). **C,** After 4 hours, cocultures of healthy donor $CD34^+$ cells with either unmodified or MSLN CAR T cells at 2:1 E:T ratio were transferred to methylcellulose with cytokines for CFC assay. Colonies derived from erythroid (E), granulocyte-macrophage (G, M, and GM) and multipotential granulocyte, erythroid, macrophage, megakaryocyte (GEMM) progenitors were scored and enumerated after 7–10 days. Data are presented as mean ± SD from three technical replicates for each donor. No significant difference in the total number of colonies was detected between cocultures with unmodified T cells versus MSLN CAR T cells as determined by unpaired Student *t* test, assuming unequal variances.

soluble MSLN, and enhanced cytotoxicity of anti-MSLN–targeted therapies. We therefore asked whether modulating MSLN shedding can improve the efficacy of MSLN CAR T cells. Treatment of Nomo-1 cells with GM6001 increased the level of cell surface MSLN (**Fig. 6A**) and caused a corresponding reduction in soluble MSLN in the culture supernatant (**Fig. 6B**), suggesting that GM6001 treatment stabilizes MSLN on the cell surface. Furthermore, GM6001 treatment of Nomo-1 cells enhanced the cytolytic activity and cytokine production of MSLN CAR T cells (**Fig. 6C–E**), but did not significantly impact cell viability after 48 hours of exposure (Supplementary Fig. S9) or alter the cytolytic activity of unmodified T cells (**Fig. 6C**). These results demonstrate the utility of inhibiting MSLN shedding to improve CAR T-cell functionality.

We attempted to extend our *in vitro* analysis of the effect of GM6001 on MSLN expression and CAR T-cell efficacy to an *in vivo* model. We found that administration of GM6001 intraperitoneally once a day for 3–7 days did not result in detectably increased levels of surface expression of MSLN on Nomo-1 cells in the mice (**Fig. 6F–H**), and therefore did not pursue this further. GM6001 is known to be quickly degraded *in vivo* (half-life < 15 minutes; ref. 14; see also Material and Methods), which probably explains the difference between its effects in cell culture and a physiologic model system. The *in vitro* results do suggest that it may be possible to increase CAR T-cell efficacy by increasing MSLN antigen density using other strategies.

Discussion

The identification of AML-specific antigens for therapeutic targeting with CAR T cells has been elusive due to genomic and phenotypic heterogeneity as well as overlapping cell surface expression with normal hematopoiesis. We have addressed this obstacle by conducting a comprehensive discovery effort in AML thus far that enabled us to define a library of CAR targets that are silent in normal hematopoiesis but highly expressed in AML, providing an opportunity to devise highly specific immunotherapies that will uniquely target leukemic cells without impacting normal hematopoiesis. In this study, we prioritized one of these targets for therapeutic development in AML, MSLN. We previously demonstrated the expression of MSLN in pediatric and adult AML as well as therapeutic targeting with antibody–drug conjugates (7). Here, we report MSLN expression in LSCs and the preclinical efficacy of MSLN CAR T cells in eradicating AML cells *in vitro* and *in vivo* without any cytotoxicity against normal HSPCs. Furthermore, CAR T-cell functionality can be improved by inhibiting MSLN shedding and stabilizing MSLN on the cell surface.

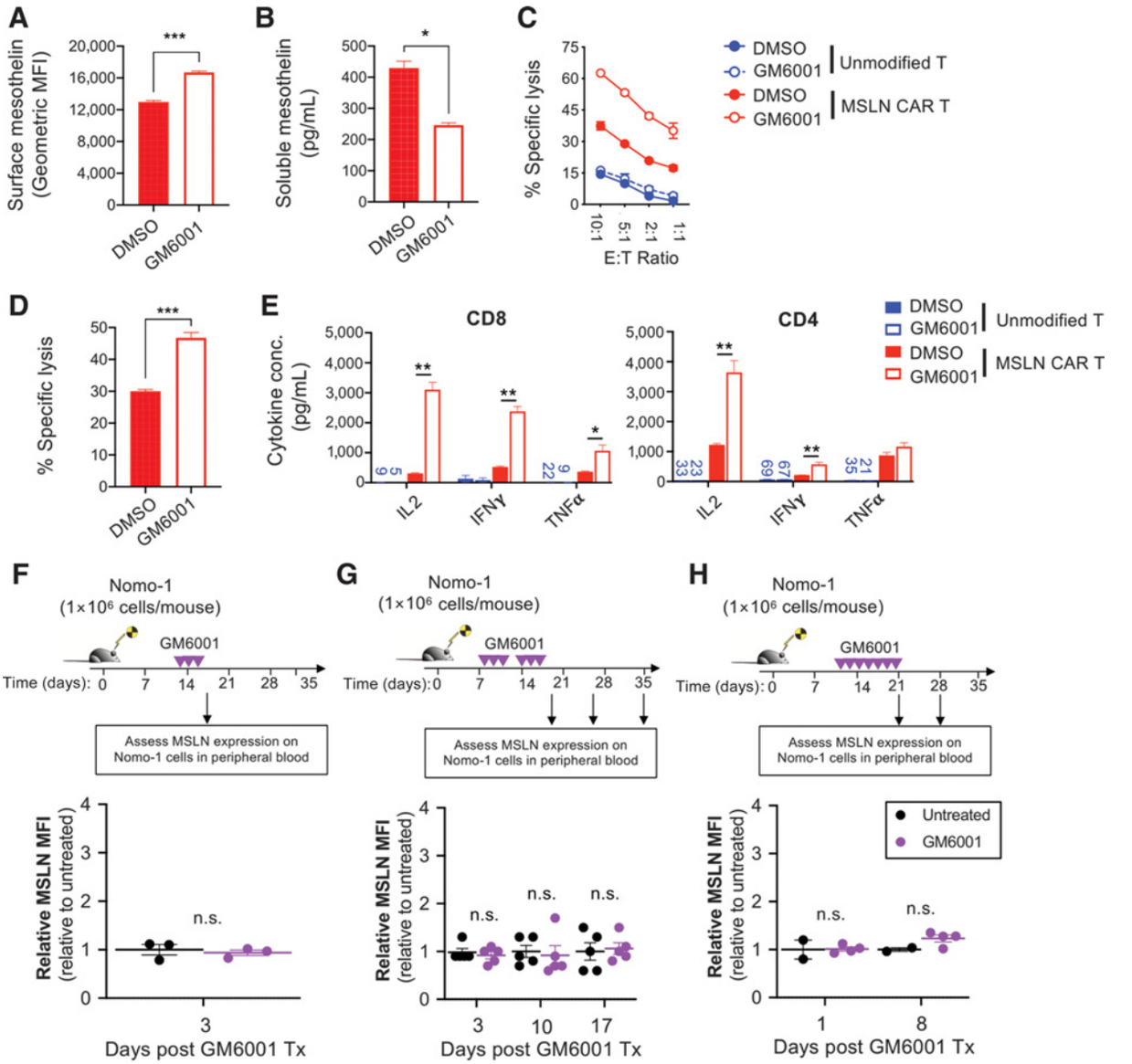

Figure 6.

Inhibiting ADAM17-mediated MSLN shedding enhances activity of CAR T cells. **A** and **B,** Quantification of flow cytometry analysis of cell surface MSLN levels (**A**) and ELISA analysis of soluble MSLN in culture supernatant (**B**) of Nomo-1 cells incubated with GM6001 (50 μmol/L) or DMSO for 48 hours. Data presented are the average ± SEM from three independent experiments. **C,** Cytolytic activity of CD8 MSLN CAR T cells against Nomo-1 in the presence of GM6001 (50 μmol/L) or DMSO. Shown is the mean leukemia specific lysis ± standard deviation from three technical replicates at each E:T ratio. **D,** Experiment shown in **C** was repeated twice, each using T cells from a different donor. Shown is the mean leukemia specific lysis ± SEM from three independent experiments at 5:1 E:T ratio. **E,** Concentration of secreted IL2, IFNγ, and TNFα in the supernatant following 10 hours of CD8 MSLN CAR T-cell/Nomo-1 and CD4 MSLN CAR T-cell/Nomo-1 coculture at 10:1 E:T ratio in the presence of GM6001 (50 μmol/L) or DMSO as measured by ELISA. Data presented are representative of 2 donors with mean ± SD from three technical replicates. **C–E,** Nomo-1 cells was pretreated with either GM6001 (50 μmol/L) or DMSO for 48 hours prior to coincubation with T cells. **A–E,** Statistical significance was determined by unpaired Student *t* test, assuming unequal variances. $P < 0.05$ (*), $P < 0.005$ (**), $P < 0.0005$ (***). **F–H,** GM6001 did not affect surface expression of MSLN on Nomo-1 cells *in vivo*. Top, experimental schema showing injection of Nomo-1 cells into NSG mice followed by treatment of transplanted mice with GM6001 (100 mg/kg i.p. injection once a day) at various dosing regimens. Bottom, surface expression of MSLN on Nomo-1 cells post GM6001 treatment was assessed by flow cytometric analysis of peripheral blood drawn by retro-orbital bleeds. Statistical significance was determined by unpaired Student *t* test, assuming unequal variances.

Thus, MSLN is a viable target for immunotherapeutic targeting with CAR T-cell therapy in AML.

MSLN represents a promising target in AML as both transcript and flow cytometry data show high expression in a subset of AML but no expression in normal HSPCs. Given that it is expressed in limited number of tissues (mesothelial cells lining the pleura, pericardium, and peritoneum; ref. 27), initial clinical trials with MSLN CAR T cells tested for solid tumors showed very minimal toxicity without cytokine release syndrome (28–31). Relevant to our work, three phase I clinical trials (University of Pennsylvania:

NCT01355965, NCT01897415, NCT02159716) used CD3zeta/41-BB-based CAR with scFv derived from SS1P and demonstrated that the MSLN-directed CAR T cells were well tolerated without pericarditis, pleuritis, and peritonitis (28–30). To assess potential impact on normal hematopoiesis, we evaluated the cytolytic activity of MSLN CAR T cells against normal HSCs and found that the viability of HSCs and early progenitors remain intact when they are coincubated with CAR T cells. Furthermore, MSLN CAR T cells did not compromise the self-renewal and multilineage differentiation capacity of HSPCs. This finding is anticipated given that MSLN is not expressed in the HSPC compartment and further supports the hypothesis that targeting MSLN in AML with CAR T cells may be safe and well tolerated.

Targeting LSCs is considered the "holy grail" of antileukemia treatment as these cells resist chemotherapy and can reinitiate disease after treatment (32). Here, we show that MSLN is expressed on LSC-enriched $CD34^+CD38^-$ subset and that these cells can be eradicated by MSLN CAR T cells. Although samples with low/intermediate MSLN expression (patients 1 and 2) elicited similar cytotoxicity compared to samples with high MSLN expression, cytokine production of CAR T cells was only moderately induced in these samples (**Fig. 4C**), suggesting a threshold level of MSLN expression is required for efficient CAR T-cell activity. If antigen density proves to impact CAR efficacy and signaling, strategies to enhance MSLN expression in LSCs would further improve CAR T-cell recognition of these cells. We have previously reported that MSLN expression in AML is associated with promoter hypomethylation (7), as it is in solid tumors (33–35). Thus, treatment with epigenetic-modifying agents may improve CAR T-cell efficacy, and the ability of these agents to enhance MSLN expression in LCSs should be evaluated. In addition, inhibiting MSLN shedding by blocking ADAM17 metalloprotease can also increase the cell surface density of MSLN. Finally, modifying CAR elements including scFv binding and signaling components (i.e., CD28z) can increase antileukemic sensitivity and efficacy (36), especially against LSCs with low antigen density.

In this study, we demonstrate potent, target-dependent cytotoxicity of MSLN CAR T cells against a variety of AML cell lines and patient samples characterized by various levels of MSLN expression. Importantly, we show that MSLN CAR T cells were effective in eradicating the leukemia as evident in the KMT2A-rearranged–positive PDX model after injecting 1×10^7 T cells per mouse. However, the mice that received a lower T-cell dose of 5×10^6 cells per mouse eventually relapsed with extramedullary disease (chloromas), a clinical feature that is prevalent in KMT2A-rearranged leukemias and poses a substantial therapeutic challenge (37). We have previously demonstrated a significant correlation between MSLN expression and EMD (7). Given that MSLN is implicated in mediating cell adhesion (38), we hypothesize that MSLN expression promotes chloroma formation, which in turn enables CAR T-cell evasion and reinitiation of the disease. Although CAR T-cell therapy has shown efficacy against extramedullary acute lymphoid leukemia (39), its activity against EMD in the setting of AML has not been fully investigated. Additional work is required to understand the role of MSLN in AML pathobiology, specifically in EMD, and define strategies to eliminate EMD and enhance CAR T-cell efficacy.

Another potential barrier to effective CAR T-cell therapeutic targeting of MSLN in AML is that MSLN is shed from the cell surface. Although soluble MSLN (the product of shedding) can be used as a biomarker for detection and diagnosis (40–43), with demonstrated utility for disease monitoring in AML (7), shedding can compromise CAR T-cell efficacy by reducing antigen site density and possibly promoting dissociation of CAR T/leukemia cell interaction as similar inhibitory effects of shedding were observed with MSLN-targeting SS1P immunotoxin (19–21). In addition, soluble antigen may abrogate CAR T-cell function by blocking their antigen-binding domain. This is documented for BCMA CAR T cells for multiple myeloma where high concentrations of soluble BCMA (333–1,000 ng/mL) impair CAR T-cell recognition and cytolytic activity (44). Of note, however, clinical trials of BCMA CAR T cells show absence of correlation between soluble BCMA concentrations and extent of response (45–47), perhaps due to different BCMA CAR T cells directed to distinct epitopes. In this study, we demonstrated that the inhibitory effects of shedding can be overcome by treatment with GM6001, which inhibits the ADAM17 metalloprotease responsible for MSLN shedding. GM6001 treatment resulted in an increased level of cell surface MSLN, a decreased level of soluble MSLN, and enhanced leukemia killing capacity of CAR T cells. Although GM6001 was active *in vitro*, it did not significantly increase the surface expression of MSLN *in vivo*, possibly due to short systemic half-life of GM6001 (<15 minutes; ref. 14; see also Materials and Methods). Nonetheless, these results suggest that inhibition of ADAM17 may be an effective strategy to improve efficacy of MSLN-directed CAR T cells. While ADAM17 inhibitors are not currently in use in the clinic, a new small molecule INCB7839, which inhibits both ADAM10 and ADAM17 proteases, has demonstrated preclinical and clinical efficacy in combination with trastuzumab in metastatic HER2 breast cancer (48, 49) and is currently under clinical investigation for children with recurrent or progressive high-grade gliomas (NCT04295759). It will be useful to evaluate potential synergy between INCB7839 and MSLN CAR T cells in AML. Alternatively, selection of scFvs that bind to the extracellular region of MSLN that remains after cleavage would circumvent the inhibitory effects of shedding.

Although mature clinical data have yet to be published, several case studies report feasibility, but suboptimal response with CAR T cells targeting lineage markers CD33 and CD123 in AML. As such lineage-directed CAR T cells cannot differentiate between leukemic and normal myeloid cells, effective targeting of these markers would lead to prolonged myelosuppression or myeloablation, requiring elimination of the CAR T cells and/or stem cell transplant to restore hematopoiesis within short few weeks after CAR T cells, which would limit surveillance and as a result its efficacy. As MSLN is not expressed in normal hematopoiesis, it would permit long-term persistence of the CAR T cells and enhanced efficacy. In addition, MSLN CAR T cells can be used as postchemotherapy or posttransplant maintenance to minimize relapse. The results presented here have successfully addressed a fundamental impediment to effective immunotherapy in AML by defining and validating MSLN as an AML-restricted target for CAR T-cell development. The ability of MSLN CAR T cells to effectively kill AML cells without impacting the viability of normal HPSCs provides the preclinical foundation for further evaluation of MSLN-directed CAR T cells in clinical trials for AML.

Authors' Disclosures

S. Srivastava reports grants and personal fees from Lyell Immunopharma outside the submitted work; in addition, S. Srivastava has a patent for PCT/US2018/049812 licensed and with royalties paid from Lyell Immunopharma and a patent for PCT/US2018/056796 licensed and with royalties paid from Bristol-Myers Squibb. M.R. Loken reports grants from NCI during the conduct of the study, as well as other support from Hematologics, Inc outside the submitted work; M.R. Loken also has equity ownership at Hematologics, Inc. C. Correnti reports other support from Link Immunotherapeutics, Inc. outside the submitted work; in addition, C. Correnti has a provisional patent on a novel mesothelin antibody not described in this work pending. S. Fiorenza reports grants from Bristol Myers Squibb and other support from Link Immunotherapeutics outside the submitted work; in addition, S. Fiorenza has a patent

for PCT/US2021/025255 issued, a patent for PCT/US2021/025248 issued, and a patent for PCT/US2021/025260 issued, licensed, and with royalties paid from Bristol Myers Squibb. C.J. Turtle reports grants from NCI during the conduct of the study. C.J. Turtle also reports grants from Juno/BMS and TCR2; personal fees and other support from Precision Biosciences, Caribou Biosciences, Myeloid Therapeutics, and Arsenal Bio; grants and personal fees from Nektar Therapeutics and AstraZeneca; other support from Eureka Therapeutics and T-CURX; and personal fees from Century Therapeutics, Allogene, Aptevo, Asher Bio, Amgen, and Humanigen outside the submitted work. S. Riddell reports grants and personal fees from Lyell Immunopharma outside the submitted work, as well as patents licensed to Bristol Myers Squibb and to Lyell Immunopharma. No disclosures were reported by the other authors.

Authors' Contributions

Q. Le: Conceptualization, resources, data curation, formal analysis, supervision, validation, investigation, visualization, methodology, writing–original draft, writing–review and editing. **S. Castro:** Data curation, investigation, methodology. **T. Tang:** Investigation. **A.M. Loeb:** Investigation. **T. Hylkema:** Investigation. **C.N. McKay:** Investigation. **L. Perkins:** Resources, investigation, methodology. **S. Srivastava:** Writing–review and editing. **L. Call:** Data curation, investigation. **J. Smith:** Data curation, formal analysis. **A. Leonti:** Formal analysis. **R. Ries:** Resources. **L. Pardo:** Investigation. **M.R. Loken:** Writing–review and editing. **C. Correnti:** Writing–review and editing. **S. Fiorenza:** Conceptualization, resources, methodology, writing–review and editing. **C.J. Turtle:** Conceptualization, resources, methodology, writing–review and editing. **S. Riddell:** Writing–review and editing. **K. Tarlock:** Writing–review and editing. **S. Meshinchi:** Conceptualization, supervision, funding acquisition, writing–review and editing.

Acknowledgments

This study was supported by LLS and St. Baldrick's Foundation.

The costs of publication of this article were defrayed in part by the payment of page charges. This article must therefore be hereby marked *advertisement* in accordance with 18 U.S.C. Section 1734 solely to indicate this fact.

Received May 3, 2021; revised June 26, 2021; accepted August 5, 2021; published first August 11, 2021.

References

1. Tarlock K, Meshinchi S. Pediatric acute myeloid leukemia: biology and therapeutic implications of genomic variants. Pediatr Clin North Am 2015;62:75–93.
2. Pui CH, Carroll WL, Meshinchi S, Arceci RJ. Biology, risk stratification, and therapy of pediatric acute leukemias: an update. J Clin Oncol 2011;29:551–65.
3. Arceci RJ. S. M. Biology of acute myeloid leukemia. In: Reaman G, Smith FO, editors. Childhood Leukemia. 2011.
4. June CH, Sadelain M. Chimeric antigen receptor therapy. N Engl J Med 2018;379:64–73.
5. Fry TJ, Shah NN, Orentas RJ, Stetler-Stevenson M, Yuan CM, Ramakrishna S, et al. CD22-targeted CAR T cells induce remission in B-ALL that is naive or resistant to CD19-targeted CAR immunotherapy. Nat Med 2018;24:20–8.
6. Mardiana S, Gill S. CAR T cells for acute myeloid leukemia: state of the art and future directions. Front Oncol 2020;10:697.
7. Kaeding AJ, Barwe SP, Gopalakrishnapillai A, Ries RE, Alonzo TA, Gerbing RB, et al. Mesothelin is a novel cell surface disease marker and potential therapeutic target in acute myeloid leukemia. Blood Adv 2021;5:2350–61.
8. Le DT, Wang-Gillam A, Picozzi V, Greten TF, Crocenzi T, Springett G, et al. Safety and survival with GVAX pancreas prime and Listeria Monocytogenes-expressing mesothelin (CRS-207) boost vaccines for metastatic pancreatic cancer. J Clin Oncol 2015;33:1325–33.
9. Weekes CD, Lamberts LE, Borad MJ, Voortman J, McWilliams RR, Diamond JR, et al. Phase I study of DMOT4039A, an antibody-drug conjugate targeting mesothelin, in patients with unresectable pancreatic or platinum-resistant ovarian cancer. Mol Cancer Ther 2016;15:439–47.
10. Beatty GL, Haas AR, Maus MV, Torigian DA, Soulen MC, Plesa G, et al. Mesothelin-specific chimeric antigen receptor mRNA-engineered T cells induce anti-tumor activity in solid malignancies. Cancer Immunol Res 2014;2:112–20.
11. Le DT, Brockstedt DG, Nir-Paz R, Hampl J, Mathur S, Nemunaitis J, et al. A live-attenuated Listeria vaccine (ANZ-100) and a live-attenuated Listeria vaccine expressing mesothelin (CRS-207) for advanced cancers: phase I studies of safety and immune induction. Clin Cancer Res 2012;18:858–68.
12. Turtle CJ, Hanafi LA, Berger C, Hudecek M, Pender B, Robinson E, et al. Immunotherapy of non-Hodgkin's lymphoma with a defined ratio of CD8+ and CD4+ CD19-specific chimeric antigen receptor-modified T cells. Sci Transl Med 2016;8:355ra116.
13. Chowdhury PS, Viner JL, Beers R, Pastan I. Isolation of a high-affinity sSupplementary table single-chain Fv specific for mesothelin from DNA-immunized mice by phage display and construction of a recombinant immunotoxin with anti-tumor activity. Proc Natl Acad Sci U S A 1998;95:669–74.
14. Bohm G, Groll J, Heffels KH, Heussen N, Ink P, Alizai HP, et al. Influence of MMP inhibitor GM6001 loading of fibre coated polypropylene meshes on wound healing: Implications for hernia repair. J Biomater Appl 2018;32:1343–59.
15. Turtle CJ, Hanafi LA, Berger C, Gooley TA, Cherian S, Hudecek M, et al. CD19 CAR-T cells of defined CD4+:CD8+ composition in adult B cell ALL patients. J Clin Invest 2016;126:2123–38.
16. Hudecek M, Sommermeyer D, Kosasih PL, Silva-Benedict A, Liu L, Rader C, et al. The nonsignaling extracellular spacer domain of chimeric antigen receptors is decisive for in vivo antitumor activity. Cancer Immunol Res 2015;3:125–35.
17. Guest RD, Hawkins RE, Kirillova N, Cheadle EJ, Arnold J, O'Neill A, et al. The role of extracellular spacer regions in the optimal design of chimeric immune receptors: evaluation of four different scFvs and antigens. J Immunother 2005;28:203–11.
18. Rosskopf S, Leitner J, Paster W, Morton LT, Hagedoorn RS, Steinberger P, et al. A Jurkat 76 based triple parameter reporter system to evaluate TCR functions and adoptive T cell strategies. Oncotarget 2018;9:17608–19.
19. Awuah P, Bera TK, Folivi M, Chertov O, Pastan I. Reduced shedding of surface mesothelin improves efficacy of mesothelin-targeting recombinant immunotoxins. Mol Cancer Ther 2016;15:1648–55.
20. Pak Y, Zhang Y, Pastan I, Lee B. Antigen shedding may improve efficiencies for delivery of antibody-based anticancer agents in solid tumors. Cancer Res 2012;72:3143–52.
21. Zhang Y, Chertov O, Zhang J, Hassan R, Pastan I. Cytotoxic activity of immunotoxin SS1P is modulated by TACE-dependent mesothelin shedding. Cancer Res 2011;71:5915–22.
22. Pastan I, Zhang Y. Modulating mesothelin shedding to improve therapy. Oncotarget 2012;3:114–5.
23. Garcia-Guerrero E, Sierro-Martinez B, Perez-Simon JA. Overcoming chimeric antigen receptor (CAR) modified T-cell therapy limitations in multiple myeloma. Front Immunol 2020;11:1128.
24. Lichtenthaler SF, Lemberg MK, Fluhrer R. Proteolytic ectodomain shedding of membrane proteins in mammals-hardware, concepts, and recent developments. EMBO J 2018;37:e99456.
25. Van Schaeybroeck S, Kyula JN, Fenton A, Fenning CS, Sasazuki T, Shirasawa S, et al. Oncogenic Kras promotes chemotherapy-induced growth factor shedding via ADAM17. Cancer Res 2011;71:1071–80.
26. Kyula JN, Van Schaeybroeck S, Doherty J, Fenning CS, Longley DB, Johnston PG. Chemotherapy-induced activation of ADAM-17: a novel mechanism of drug resistance in colorectal cancer. Clin Cancer Res 2010;16:3378–89.
27. Hassan R, Thomas A, Alewine C, Le DT, Jaffee EM, Pastan I. Mesothelin immunotherapy for cancer: ready for prime time? J Clin Oncol 2016;34:4171–9.
28. Beatty GL, O'Hara MH, Lacey SF, Torigian DA, Nazimuddin F, Chen F, et al. Activity of mesothelin-specific chimeric antigen receptor T cells against pancreatic carcinoma metastases in a phase 1 trial. Gastroenterology 2018;155:29–32.
29. Haas AR, Tanyi JL, O'Hara MH, Gladney WL, Lacey SF, Torigian DA, et al. Phase I study of lentiviral-transduced chimeric antigen receptor-modified T cells recognizing mesothelin in advanced solid cancers. Mol Ther 2019;27:1919–29.

30. Maus MV, Haas AR, Beatty GL, Albelda SM, Levine BL, Liu X, et al. T cells expressing chimeric antigen receptors can cause anaphylaxis in humans. Cancer Immunol Res 2013;1:26–31.
31. Adusumilli PS, Zauderer MG, Rusch VW, O'Cearbhaill RE, Zhu A, Ngai DA, et al. A Phase I clinical trial of malignant pleural disease treated with regionally delivered autologous mesothelin-targeted CAR T cells: safety and efficacy. American Association for Cancer Research Annual Meeting. 2019.
32. Bruserud O, Aasebo E, Hernandez-Valladares M, Tsykunova G, Reikvam H. Therapeutic targeting of leukemic stem cells in acute myeloid leukemia - the biological background for possible strategies. Expert Opin Drug Discov 2017;12:1053–65.
33. Nelson HH, Almquist LM, LaRocca JL, Plaza SL, Lambert-Messerlian GM, Sugarbaker DJ, et al. The relationship between tumor MSLN methylation and serum mesothelin (SMRP) in mesothelioma. Epigenetics 2011;6:1029–34.
34. Hollevoet K, Mason-Osann E, Muller F, Pastan I. Methylation-associated partial down-regulation of mesothelin causes resistance to anti-mesothelin immunotoxins in a pancreatic cancer cell line. PLoS One 2015;10:e0122462.
35. Liu XF, Zhou Q, Hassan R, Pastan I. Panbinostat decreases cFLIP and enhances killing of cancer cells by immunotoxin LMB-100 by stimulating the extrinsic apoptotic pathway. Oncotarget 2017;8:87307–16.
36. Rafiq S, Hackett CS, Brentjens RJ. Engineering strategies to overcome the current roadblocks in CAR T cell therapy. Nat Rev Clin Oncol 2020;17:147–67.
37. Tarlock K, Alonzo T, Gerbing R, Le Q, Kolb E, Meshinchi S. Mesothelin expression is associated with extramedullary disease and promotes in vivo leukemic growth in acute myeloid leukemia. Blood 2020; American Society of Hematology Annual Meeting.
38. Tsai JM, Sinha R, Seita J, Fernhoff N, Christ S, Koopmans T, et al. Surgical adhesions in mice are derived from mesothelial cells and can be targeted by antibodies against mesothelial markers. Sci Transl Med 2018;10:eaan6735.
39. Zhang H, Hu Y, Wei G, Wu W, Huang H. Successful chimeric antigen receptor T cells therapy in extramedullary relapses of acute lymphoblastic leukemia after allogeneic hematopoietic stem cell transplantation. Bone Marrow Transplant 2020;55:1476–8.
40. Baldo P, Cecco S. Amatuximab and novel agents targeting mesothelin for solid tumors. Onco Targets Ther 2017;10:5337–53.
41. Gao R, Wang F, Wang Z, Wu Y, Xu L, Qin Y, et al. Diagnostic value of soluble mesothelin-related peptides in pleural effusion for malignant pleural mesothelioma: an updated meta-analysis. Medicine (Baltimore) 2019;98:e14979.
42. Ho M, Onda M, Wang QC, Hassan R, Pastan I, Lively MO. Mesothelin is shed from tumor cells. Cancer Epidemiol Biomarkers Prev 2006;15:1751.
43. Madeira K, Dondossola ER, Farias BF, Simon CS, Alexandre MC, Silva BR, et al. Mesothelin as a biomarker for ovarian carcinoma: a meta-analysis. An Acad Bras Cienc 2016;88:923–32.
44. Pont MJ, Hill T, Cole GO, Abbott JJ, Kelliher J, Salter AI, et al. gamma-Secretase inhibition increases efficacy of BCMA-specific chimeric antigen receptor T cells in multiple myeloma. Blood 2019;134:1585–97.
45. Cohen AD, Garfall AL, Stadtmauer EA, Lacey SF, Lancaster E, Vogl DT, et al. Safety and efficacy of B-cell maturation antigen (BCMA)-specific chimeric antigen receptor T cells (CART-BCMA) with cyclophosphamide conditioning for refractory multiple myeloma (MM). Blood 2017;130:505.
46. Brudno JN, Maric I, Hartman SD, Rose JJ, Wang M, Lam N, et al. T cells genetically modified to express an anti-B-cell maturation antigen chimeric antigen receptor cause remissions of poor-prognosis relapsed multiple myeloma. J Clin Oncol 2018;36:2267–80.
47. Berdeja JG, Lin Y, Raje N, Munshi N, Siegel D, Liedtke M, et al. Durable clinical responses in heavily pretreated patients with relapsed/refractory multiple myeloma: updated results from a Multicenter Study of bb2121 anti-Bcma CAR T cell therapy. Blood 2017;130:740.
48. Friedman S, Levy R, Garrett W, Doval D, Bondarde S, Sahoo T, et al. Clinical benefit of INCB7839, a potent and selective inhibitor of ADAM10 and ADAM17, in combination with trastuzumab in metastatic HER2 positive breast cancer patients. Cancer Res 2009;69(24_suppl):5056.
49. Witters L, Scherle P, Friedman S, Fridman J, Caulder E, Newton R, et al. Synergistic inhibition with a dual epidermal growth factor receptor/HER-2/neu tyrosine kinase inhibitor and a disintegrin and metalloprotease inhibitor. Cancer Res 2008;68:7083–9.